

## Synthesis of Novel Fibrous Cerium Phosphate-Silver-Polyethylene Nanocomposites for Antibacterial Applications

S. K. Shakshooki\*

Department of Chemistry, Faculty of Science, University of Tripoli, Tripoli, Libya

N. Greesh

Advanced laboratory for Chemical Analysis, Tripoli, Libya

R. Alghazeer

Department of Chemistry, Faculty of Science, University of Tripoli, Tripoli, Libya

F. Hebail

Faculty of Education, University of Tripoli, Janzur, Tripoli, Libya

A. Elhamadi

Advanced laboratory for Chemical Analysis, Tripoli, Libya

A. Elouzi

Department of Chemistry, Faculty of Science, University of Tripoli, Tripoli, Libya

W. Elharari

Polymer Research Center, Tripoli, Libya

A. Shebani

Polymer Research Center, Tripoli, Libya

**Abstract:** Fibrous cerium phosphate silver nanocomposite,  $Ce(H)_{0.7}(PO_4)_2(Ag)_{1.3} \cdot 2.97H_2O(CePAg)$ , was prepared by ion exchange method from reaction of  $Ce(HPO_4)_2 \cdot 2.9H_2O(nCeP_f)$  with  $0.1M AgNO_3$  in  $0.1M HNO_3$  solution. Fibrous cerium phosphate-silver nanocomposite(CePAg) was dispersed in polyethylene by melt process using twin extruder at different loading : 2, 5 and 10 % in wt., with respect to polyethylene(PE), to obtain cerium phosphate-silver-polyethylene nanocomposites (CePAg-PE). The resultant products were characterized by FTIR, XRD, SEM and TGA. The antimicrobial resistance of CePAg-PE was studied by measuring the diameter of inhibition zone of growths of Escherichia coli and Salmonella typhimurium. The results showed that CePAg-PE exhibited efficacy in the inhibition of bacterial growth especially at 10 w% content.

**Keywords:** Fibrous cerium phosphate-silver; Polyethylene nanocomposites; Antibacterial.

### 1. Introduction

Tetravalent metal phosphates are very insoluble compounds with good thermal stabilities, and high ion exchange capacities [1, 2]. The discovery of their crystalline materials [3, 4], represent a fundamental step in chemistry of these compounds with general Formula  $\alpha-M(IV)(HPO_4)_2 \cdot H_2O$ , and  $\gamma-M(IV).PO_4.H_2PO_4.2H_2O$ , (where M = Ti, Zr, Hf, Ge, Sn, Ce). These materials contain structural P-OH groups with labile protons. They can exchange their protons with counter ions such as alkali, alkaline earth, transition divalent and trivalent metal ions [1-4] and act as intercalates [1, 2, 5, 6]. Increase attention direct toward their intercalation [5, 6], catalytic [7], electrical conductance [8], and sensors [9]. Layered tetravalent phosphates have potential applications as inorganic fillers, sorbents and solid acid catalysts [10-12]. This class of compounds can bond themselves to pillaring reactions by metal amine complexes exchanged in their interlayer. Successful pillaring of these type of layered materials can accomplished via amine intercalation reaction [13-17]. They can form complex pillars between the layers as its formation in-situ by ion exchange of transition metal ions and ligand intercalation. As catalysts attracted attention recently and still in their infancy [1, 2, 18-20].

Crystalline cerium phosphates have been studied for a long time as ion exchangers, their structures remains unknown until recently [21, 22]. The reason is that, the composition, the structure and the degree of crystallinity of their precipitates results from reaction of solutions containing a Ce(IV) salt which is mixed with a solution of phosphoric acid of  $[(PO_4)/Ce(IV)]$  ratio, strongly depend on the experimental conditions such as rate and order of mixing of the solutions, stirring, temperature and digestion time, this also implemented on fibrous cerium phosphate [23].

To date, most of the work on fibrous cerium phosphate was carried out on its ion exchange [24], intercalation [25] and electrical conductance properties [26]. Studies on its polystyrene, polyacrylamide [27] and (polyvinyl chloride-based polyvinyl alcohol) [28] composites have been reported. The composite material may combine the

\*Corresponding Author

advantage of each material, for instance, flexibility, processability of polymers and the selectivity and thermal stability of the inorganic filler [12, 29-33].

It has often been observed that organic polymers membranes with a hydrophilic surface are much less likely to be attached with bacteria than with hydrophobic surfaces. However, most of the industrial polymeric membrane materials are usually hydrophobic. As a result many studies focus on modifying the conventional membranes to increase their hydrophilicity so as to reduce membrane fouling [34, 35].

For antimicrobial approaches, some biocides can be directly incorporated into the membrane which aims at effectively killing bacteria that can be attached with the membrane surface and thus preventing their growth [36]. Biocides such as heavy metals including copper, or silver [37, 38] have been demonstrated for their effectiveness in anti bacterial performance. Among the silver is of special interest because is high toxicity toward many types of bacteria but low toxicity for human and animals [39, 40]. Silver nanoparticles, or ions have been incorporated to cellulose [41] polyimide [42] polyamide [43] and polysulfones [44, 45]. However, most of the work conducting in incorporating silver into polymers reported leaching problems due to poor compatibility of the silver and the polymer, [40, 41]. To overcome such losses it is necessary to design a carrier to release the silver slowly. For silver loaded inorganic antibacterial materials, the release time of silver can be delayed for a long time so that silver supported materials have great potential for antibacterial applications [42]. Several kinds of silver carriers using different inorganic carrier such as zeolites [43] mesoporous silica [44] titanium oxide [45] tetravalent metal phosphates [46] have been developed. Potential applications of hybrid composites outlined; are likely to extend, especially, to antimicrobial materials.

Antimicrobial silver mechanism the mechanisms behind the activity of composites of silver ion or silver nanoparticle (AgNPs) on bacteria are not yet fully elucidated, but the three most common mechanisms of toxicity proposed to date [30, 47-53] are: is due to its partial oxidation and release of silver ions (Ag<sup>+</sup>) [48, 49] After this oxidation occurs, the following actions can happen either simultaneously or separately: (i) Uptake of free Ag<sup>+</sup> followed by disruption of ATP production and DNA replication [49]; (ii) AgNPs and Ag<sup>+</sup> interaction with bacterial proteins, disrupting protein synthesis [30]; (iii) AgNPs directly damage cell membranes, interacting with the peptidoglycan wall cell and the plasmatic membrane causing cell lysis [50].

Besides, disregarding the exact mechanism of interaction, several works have stated that AgNPs may increase the cell membrane permeability and, subsequently, penetrate inside cells to induce any one or the entire cascade of effects just described [51-53].

Here we are reporting for the first time the preparation of polyethylene(PE) incorporated with fibrous cerium phosphate silver nanocomposite membrane (CePAg-PE), with a particular emphasis on the role of the antibacterial resistance of CePAg-PE, the antibacterial resistance studied by measuring the rate of antibacterial for four types of bacteria.

## 2. Materials and Methods

### 2.1. Chemicals

Ce(SO<sub>4</sub>)<sub>2</sub>·4H<sub>2</sub>O, H<sub>3</sub>PO<sub>4</sub>(85%) of BDH, AgNO<sub>3</sub> of Reidel De-Haen. High density polyethylene (HDPE) was used as matrix polymer (SABIC Saudi Arabia, HDPE F00952)

### 2.2. Instruments Used for Characterization

X-ray powder diffractometry Philips, using Ni-filtered CuK $\alpha$  ( $\lambda = 1.54056\text{\AA}$ ), TG/DTA Analyzer model SIIExtra6000-6300, Fourier Transform IR Spectrometer, model IFS 25 FTIR Bruker, Scanning electron microscopy (SEM) Jeol SMJ Sm 5610 LV., used for fibrous cerium phosphate, Scanning electron microscopy(SEM) LEO. used for(CePAg-PE), pH Meter WGW 52.

### 2.3. Preparation of Nanofibrous Cerium Phosphate (nCeP<sub>f</sub>)

200 ml 0.05M (CeSO<sub>4</sub>)<sub>2</sub>·4H<sub>2</sub>O in 0.5M H<sub>2</sub>SO<sub>4</sub> were added drop wise to 200ml 6M H<sub>3</sub>PO<sub>4</sub> at 80°C with stirring. The stirring was continued at that temperature for 4h. The resultant product was dispersed in 2 liter distilled water with stirring for 1h. Then subjected to washing by distilled water up to pH~3.5, filtered and allow to dry in air to obtain flexible fibrous cerium phosphate membrane.

### 2.4. Incorporation of Ag<sup>+</sup> ions Into Nanosized Fibrous Cerium Phosphate Membrane

0.273 grams of thin film nanosized fibrous cerium phosphate membrane, Ce(HPO<sub>4</sub>)<sub>2</sub>·2.9H<sub>2</sub>O, was soaked in 20ml of 0.1M AgNO<sub>3</sub> in 0.1 M HNO<sub>3</sub> solution for 72hrs. The resultant product was filtered, washed with distilled water, and left to dry in air.

The Ag<sup>+</sup> ions content were estimated gravimetrically, the water content of CeH<sub>0.7</sub>(PO<sub>4</sub>)<sub>2</sub>·(Ag<sup>+</sup>)<sub>1.3</sub>·nH<sub>2</sub>O was estimated by thermal treatment. Accordingly the loading of the silver ions and water of crystallization of the resultant material was formulated as Ce(H)<sub>0.7</sub>(PO<sub>4</sub>)<sub>2</sub>·(Ag<sup>+</sup>)<sub>1.3</sub>·2.97H<sub>2</sub>O.

## 2.5. Incorporation of $\text{CeH}_{0.7}(\text{PO}_4)_2 \cdot (\text{Ag}^+)_{1.3} \cdot 2.97\text{H}_2\text{O}$ into PET.

The HDPE of desire amount was compounded with a counter rotating twin-screw extruder at a maximum temperature of 190 °C with mixing rate 50 rpm. During melting process different amounts of CeP-Ag ( 2 , 5 and 10 wt%) relative to HDPE, were mixed with HDPE.

## 2.6. Antimicrobial Investigations

The bacterial strains listed below were authenticated and provided by the Microbiology Laboratory, Faculty of Pharmacy, University of Tripoli, Tripoli, Libya. While MRSA (clinical isolate) was obtained from Clinical Microbiology Laboratory, Tripoli Medical Center, Tripoli, Libya.

In the antibacterial property analysis [54], Gram-negative bacteria, Escherichia coli (E. coli), and Klebsiella pneumoniae (K. pneumoniae), and Gram-positive, Staphylococcus aureus (S. aureus) and Methicillin resistant Staphylococcus aureus (MRSA) bacteria were used.

The four species of bacteria were grown individually on nutrient broth (Oxoid Ltd., England) at 30 °C for 24 h, followed by the matching of bacterial suspension to the turbidity equivalent to 0.5 McFarland solution ( $1.5 \times 10^8$  CFU/mL) with the addition of sterile saline. The films were placed in sterile plate and the suspension (30 $\mu$ L) was dropped on the films. These carrier films were kept under  $37 \pm 1$  °C and relative humidity (RH) > 90%. After 24 h, the bacteria were washed off using PS and then 100 $\mu$ L serial dilution of this suspension was plated onto nutrient agar. The colony forming units (CFU) of bacteria were taken count, and the antibacterial rate (R) was calculated via the following equation;

$$R(\%) = \left[ \frac{A - B}{A} \right] \times 100$$

Where A is the CFU of blank sample and B is the CFU of antibacterial samples.

## 3. Results and Discussion

Nanosized cerium phosphate  $\text{Ce}(\text{HPO}_4)_2 \cdot 2.9\text{H}_2\text{O}(\text{nCeP}_f)$ , was prepared and characterized by chemical , XRD , TGA, FT-IR, and SEM.

### 3.1. XRD of $\text{nCeP}_f$

X-ray scattering has been widely used to characterize the layered structure of nanocomposites materials as the change in  $2\theta$  is correlated to changes in the interlayer distance nanocomposites.

X-ray diffractogram (XRD) pattern of fibrous cerium phosphate membrane is shown in Figure (1-A) with  $d_{001} = 10.85 \text{ \AA}$ .

### 3.2. FT-IR of $\text{nCeP}_f$

(Fig.1-B) shows FT-IR spectrum of fibrous cerium phosphate, with a trend similar to the IR spectra of  $\text{M}^{\text{IV}}$  phosphates. Broad band centered at  $3350 \text{ cm}^{-1}$  is due to OH groups symmetric-asymmetric stretching of  $\text{H}_2\text{O}$ , small sharp band at  $1628 \text{ cm}^{-1}$  is due to H-O-H bending, sharp broad band centered at  $1045 \text{ cm}^{-1}$  is related to phosphate groups vibration very small peak appears at  $2360 \text{ cm}^{-1}$  which related to stretching of P-O-H band.

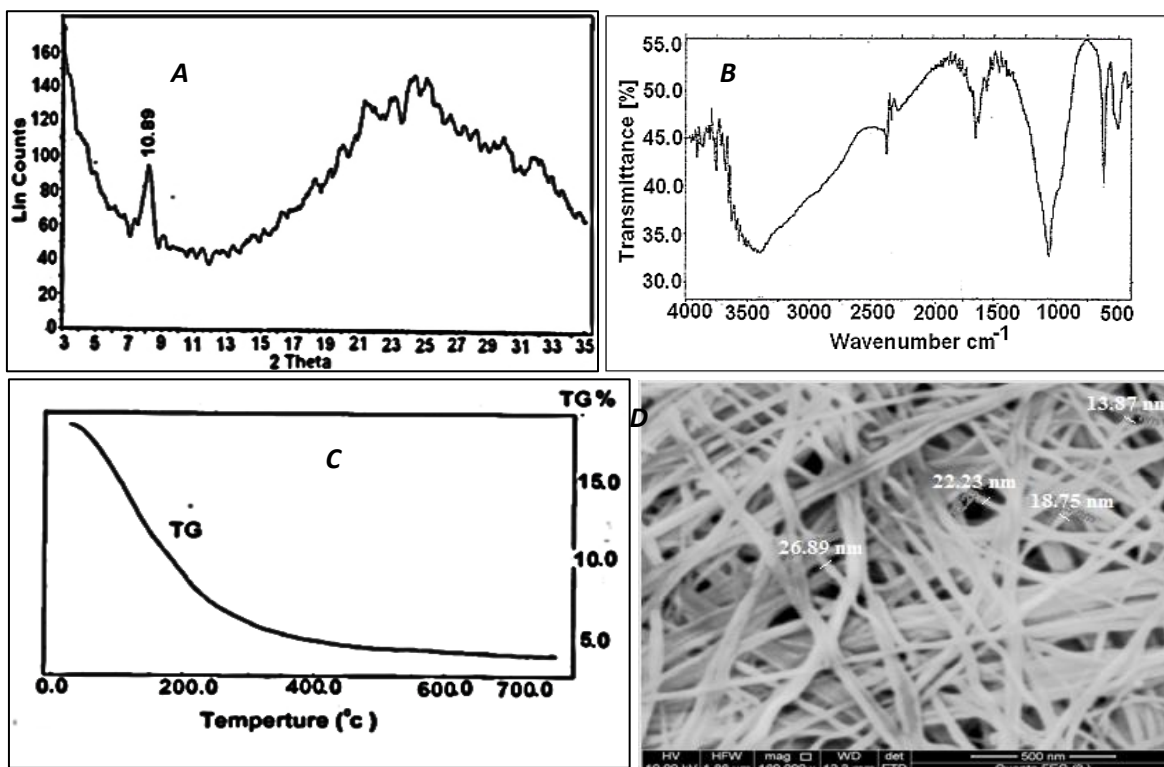
### 3.3. TGA of $\text{nCeP}_f$

Thermogram(TG) of fibrous cerium phosphate  $\text{Ce}(\text{HPO}_4)_2 \cdot 2.9\text{H}_2\text{O}$  is shown in (Fig.1-C). The thermal decomposition occurs in continuous process almost one step. The thermal analysis was carried out at temperatures between 10-750°C, the final product was  $\text{CeP}_2\text{O}_7$ , results from the loss of water of hydration between 60-200°C, followed by POH groups condensation. The total weight loss found to be equal to 19.09%.

### 3.4. SEM of $\text{nCeP}_f$

SEM image of the nanosized fibrous cerium phosphate ( $\text{nCeP}_f$ ) is shown in (Fig.1-D) Visual inspection of cerium phosphate indicated that the ( $\text{nCeP}_f$ ) was successfully obtained and a suitable as nanofibers with average size ~ 20.5 nm, which confirming that the ( $\text{nCeP}_f$ ) could be suitable as polymer nanofiller for some industrial applications.

Fig-1. Fibrous cerium phosphate : ( A ) XRD patterns ( B ) FT-IR spectrum ( C ) TGA analysis ( D ) SEM image



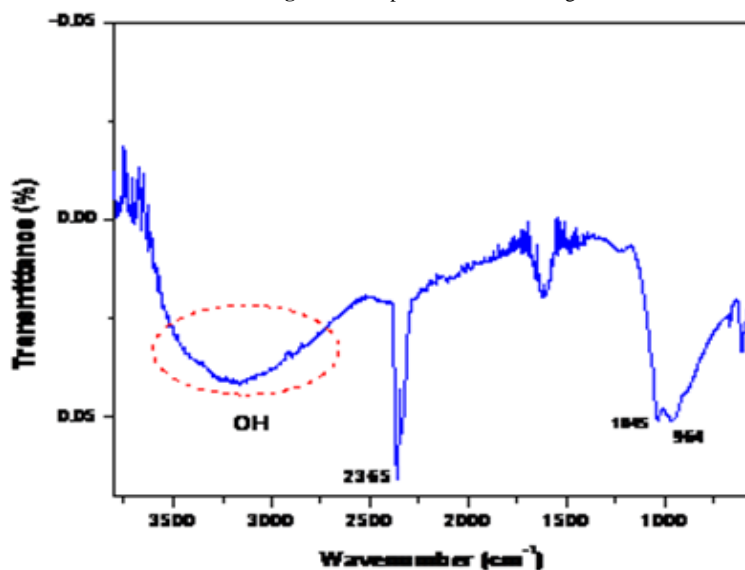
### 3.5. Exchange capacity of $n\text{CeP}_f$

The ion exchange capacity of nano fibrous cerium phosphate membrane found to be equal to 5.21 meq/g, that was determined by titration method [1, 2].

### 3.5. FT-IR of $\text{Ce}(\text{H})_{0.7}(\text{PO}_4)_2 \cdot (\text{Ag}^+)_{1.3} \cdot 2.97\text{H}_2\text{O}$ (CeP-Ag)

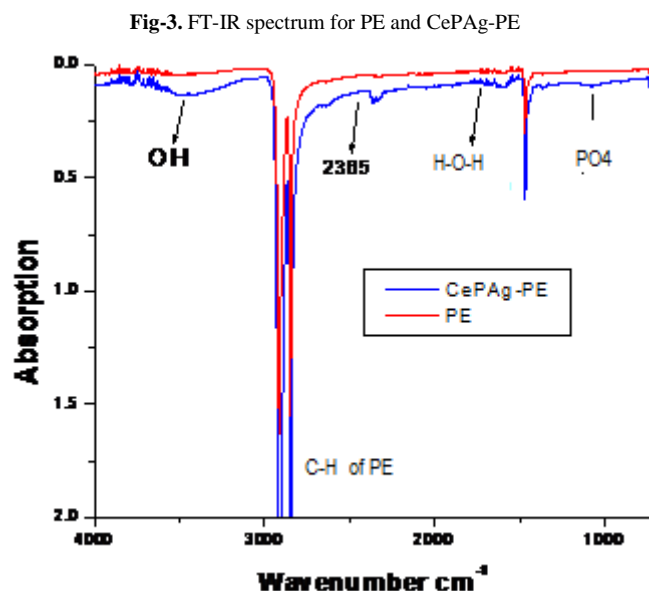
FT-IR spectrum of  $\text{Ce}(\text{H})_{0.7}(\text{PO}_4)_2 \cdot (\text{Ag}^+)_{1.3} \cdot 2.97\text{H}_2\text{O}$  is shown in (Fig. 5) and compared with FT-IR of fibrous cerium phosphate before the ion exchange process (Fig.2). The absorption bands at  $3350\text{cm}^{-1}$  is due to OH groups symmetric-asymmetric stretching of  $\text{H}_2\text{O}$ , This band shifted to a lower wavelength  $3300\text{cm}^{-1}$  in the FT-IR spectrum of  $\text{Ce}(\text{H})_{0.7}(\text{PO}_4)_2 \cdot (\text{Ag}^+)_{1.3} \cdot 2.97\text{H}_2\text{O}$  and also became broader. This is related to formation of hydrogen bonds between the OH of  $\text{Ce}(\text{HPO}_4)_2 \cdot 2.9\text{H}_2\text{O}$  and the oxygen of nitrate groups. The bands at  $\nu_1 = 962.6$  and  $\nu_2 = 1040\text{cm}^{-1}$  are assigned to the fundamental frequencies of the  $\text{PO}_4$  groups. The low intensity band at  $1630\text{cm}^{-1}$  is assigned to H-O-H bending of adsorbed water. The band observed at  $2360\text{cm}^{-1}$  is  $\text{CO}_2$  of air.

Fig-2. FT-IR spectrum for : CeP-Ag



### 3.6. FT-IR spectrum of PE, and CePAg-PE

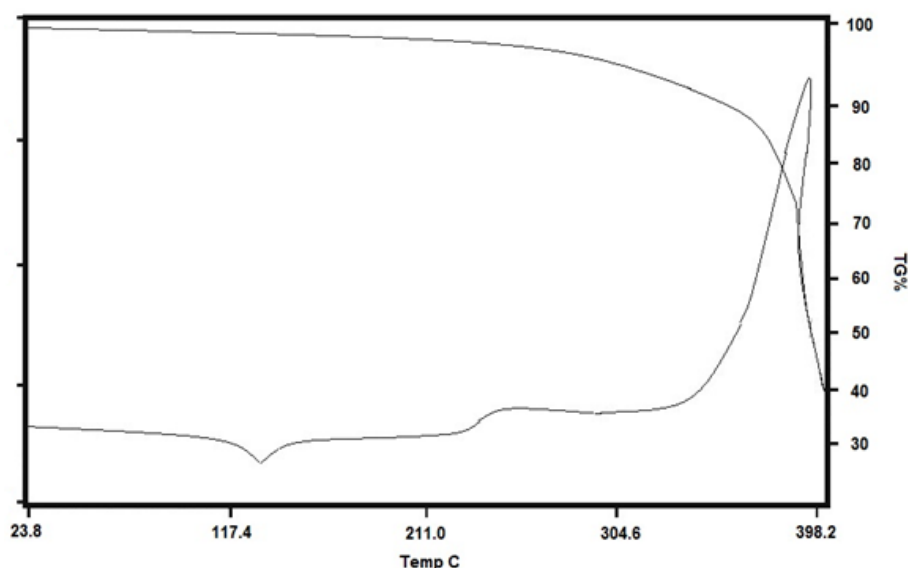
FT-IR spectrum of neat PE, and CePAg-PE were recorded, and are shown in (Fig.3). The FT-IR spectrum of PE shows absorption bands at 2850 and 2930  $\text{cm}^{-1}$ , corresponding to the C-H, stretching, [23, 24] The appearance of new bands in the FT-IR spectrum of PE incorporated with CeP-Ag ( CePAg-PE) indicates the presence of CeP-Ag in the PE. The band at 3300 $\text{cm}^{-1}$  is related to the O-H stretching adsorbed water. Sharp band(doublet) Very small band observed at 2365  $\text{cm}^{-1}$  is  $\text{CO}_2$  of air. Band at 1590 $\text{cm}^{-1}$  is corresponding to the H-O-H bending of adsorbed water. Very small broad band centered at 1015 $\text{cm}^{-1}$  can be assigned for fundamental frequencies of the  $\text{PO}_4$  groups.



### 3.7. Thermal stability of CePAg-PE

In order to gain quantitative insight into the extent to which the grafting process of CeP-Ag into PE took place, TGA was used to study thermal behavior of nanocomposites. (Fig.5) shows TG/DTA of CePAg-PE, the total loss found to be equal to 55.31 % in wt. , the residue was equal to 44.69 % in wt. The residue contain the final product of 10% in wt loading of the inorganic material  $\text{CeH}_{0.7}(\text{PO}_4)_2 \cdot (\text{Ag}^+)_{1.3} \cdot 2.97\text{H}_2\text{O}$ , which is  $\text{CeO}_2 \cdot \text{P}_2\text{O}_5 + \text{Ag}_{1.3} \text{O}_{0.65}$ .

Fig-5. Thermal stability of CeP-Ag-PE nanocomposites at 10%wt CeP-Ag loading.



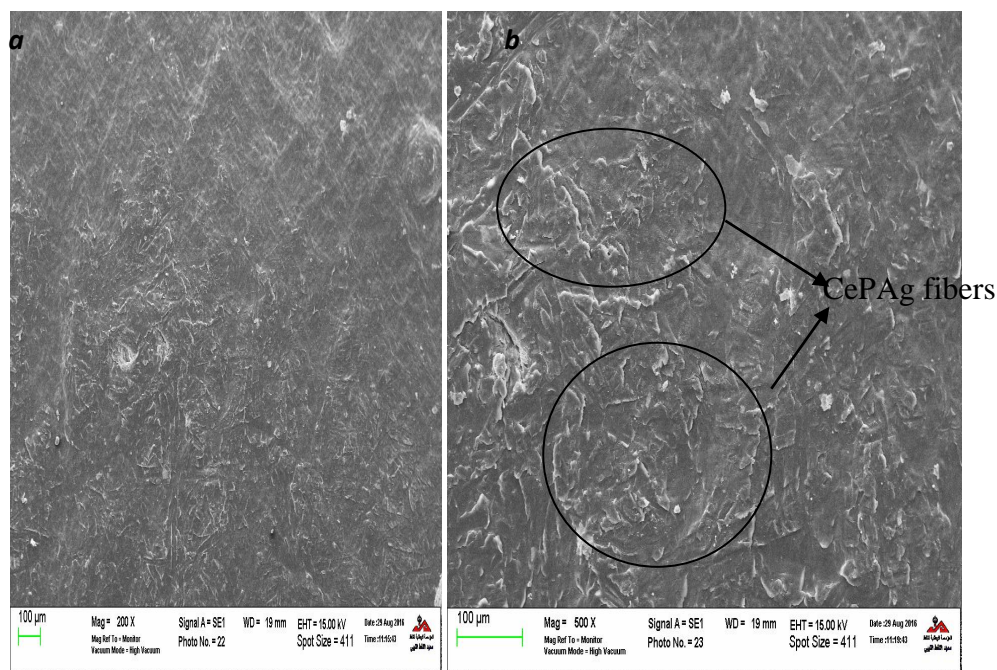
The thermal decomposition is accompanied by two endothermic peaks at about 122 and 230 $^{\circ}\text{C}$  and exothermic peak at about 398 $^{\circ}\text{C}$ . Furthermore, synthesized nanocomposites were found to be thermally more stable than neat PE, the neat PE start decomposes at 300  $^{\circ}\text{C}$  as received from SABIC, while CePAg-PE decomposed at 350  $^{\circ}\text{C}$  The improvement in thermal stability due to the presence of CePAg is probably attributed to the formation of CePAg char that acts as a mass transport barrier and as an insulator between the bulk polymer and the surface where the combustion of the polymer takes place. The presence of CePAg also hinders the diffusion of volatile decomposition

products within the nanocomposites. The enhancement of the thermal stability of nanocomposites could also attributed to the restricted thermal motion of polymer chains between CePAg nanocomposite membrane.

### 3.8. Morphology of CePAg-PE

The surface morphology of CePAg-PE was studied by SEM at different magnifications as shown in (Fig.6).

Fig-6. SEM images for CePAg-PE at different magnifications : ( a) low ( b) high

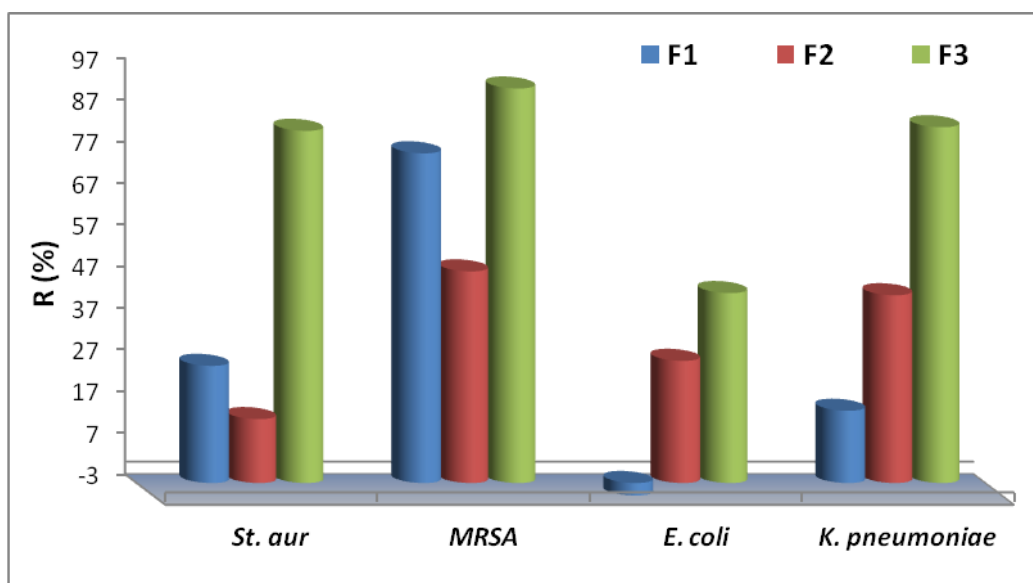


From the SEM images (Fig. 6), at low magnification show the smooth regions related to polymer. However at high magnification there are some regions of CePAg-PE appears as a light area this could be related to the presence of CePAg nanocomposite, well dispersed into PE matrix.

### 3.9. Antibacterial Property Test

Test plates of the antibacterial compounds (2%, 5% and 10 wt.% CeP-Ag) and of pristine HDPE were prepared. Antimicrobial testing was carried out following the procedure described earlier. For this assessment, gram-positive bacteria *S. aureus* as well as gram-negative bacteria *E. coli* were used. Pristine HDPE was applied as control sample in all experiments and displayed in (Fig.7).

Fig-7. Antibacterial activity of nanocomposite films against bacteria strains. *E.coli*: Escherichia coli, *K. pneumoniae*: Klebsiella pneumoniae, *St.aur*: Staphylococcus aureus. MRSA: Methicillin resistant Staphylococcus aureus: (F1) neat PE ( F2) 5% wt CeP-Ag ( F3) 10 % wt CeP-Ag

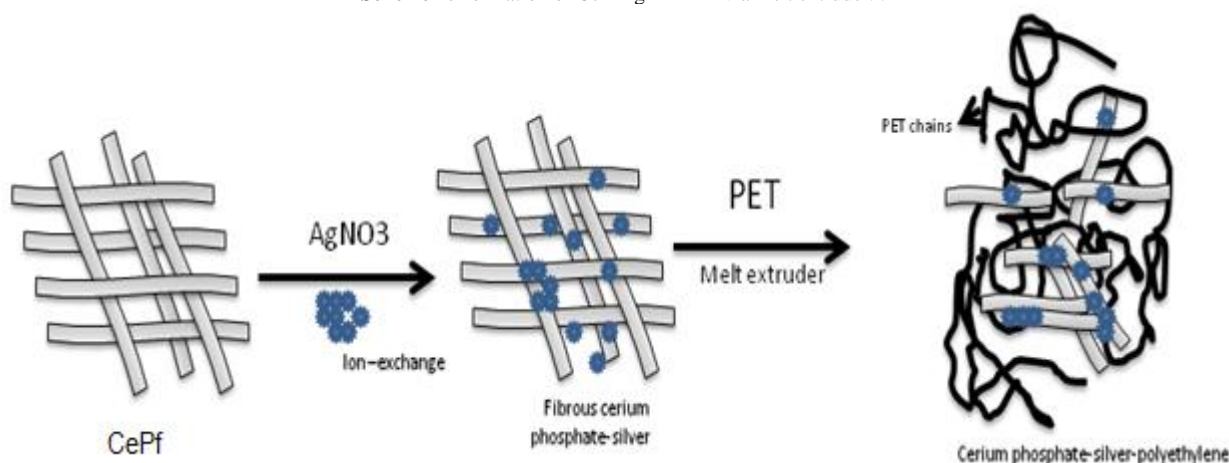


All nanocomposites found to have high rate of antibacterial relative to that of neat PE. For E. coli, the rate of antibacterial (R) was reduced to zero after a contact time of 24 h between the bacteria and the neat PE surface. On the other hand PE compounds containing CeP-Ag shows high rate of antibacterial. For all synthesized the rate of antibacterial values were high, and increased with CeP-Ag loadings, this is not surprise results since CeP-Ag contains  $\text{Ag}^+$  which play as antibacterial.

The rate of antibacterial S. aureus bacteria was also strongly increased during contact with the antimicrobial PE surfaces. The compound containing 10wt.% CeP-Ag increased rate of antibacteriales to 92%.

Based on these observations and the known mechanism of melt extruder polymerization, the mechanism by which CeP-Ag-PE film formed was proposed, shown as in Scheme 1. The melt blending process involves mixing the CeP-Ag, under shear, with the PE while heating the mixture above the softening point of the polymer. During the annealing process, the polymer chains diffuse from the bulk polymer melt between the CeP-Ag fibers.

Scheme-1. Formation of CeP-Ag-PE film via melt extruder. .



The incorporations of CeP-Ag into PE matrix ensure the presences of Ag ions into system, and these ions were not released from cerium fibers as confirmed earlier, this is resulted on PE surface has Ag ions which play a significant roles on antibacterial properties of this system.

#### 4. Conclusion

Fibrous cerium phosphate silver (CeP-Ag) nano composite membrane were synthesized by ion exchange method from reaction of  $\text{Ce}(\text{HPO}_4)_2 \cdot 2.9\text{H}_2\text{O}(\text{CeP}_f)$  with  $\text{AgNO}_3$ . Cerium phosphate -silver -polyethylene were prepared easily by compounding high density polyethylene with different loadings of CeP-Ag using twin-screw extruder. Antibacterial properties of the nanocomposites were investigated, it was found that, all nanocomposites prepared has a significant resistant against different bacterial types and increased with increasing  $\text{Ag}^+$  content in CeP-Ag composite.. CeP-Ag-PE shows slight improvement on thermal satiability relative to pure PE. This study highlights the need for further studies on the role of the CeP-Ag nanocomposites, its final morphology and antibacterial properties. This may allow chemical engineering in the near future to prepare materials with tailored properties for specific applications by fine-tuning the types of ions that ion- exchanged with fibrous cerium phosphate.

#### Acknowledgement

To Department of Chemistry, Faculty of Science, University of Tripoli, Advanced laboratory for chemical analysis, and Polymer research center, Tripoli, Libya, for providing facilities of research and analysis. To Microbiology Laboratory, Faculty of Pharmacy, University of Tripoli, and to Clinical Microbiolog Laboratory, Tripoli Medical Center, Tripoli, Libya for providing MRSA (clinical isolate).

#### References

- [1] Shakshooki, S. K., Azzabi, O. H., Khalil, S., Kowalczy, k. J., and Naqvi, N., 1988. "Crystalline mixed hafniumtitanium phosphates." *Reactive Polymers*, vol. 7, pp. 191-196.
- [2] Clearfield, A., 1982. *Inorganic Ion Exchange Materials*. 1 ed. Boca Raton, FL.US.: CRC Press.
- [3] Clearfield, A. and Styne, J. A., 1964. "The preparation of crystalline zirconium phosphate and some observation on its ion exchange behavior." *J. Inorg. Nucl. Chem.*, vol. 26, p. 117.
- [4] Alberti, G. and Torracca, E., 1968. "Synthesis of crystalline zirconium and titanium phosphate by direct precipitation." *J. Inorg. Nucl. Chem.*, vol. 30, p. 317.
- [5] Costantino, U., 1979. "Intercalation of alkanols and glycols into zirconium (IV) hydrogenphosphate monohydrate." *J.Chem.Soc. Dalton Trans*, pp. 402-406.

- [6] Vecchio, S., Di-Rocco, R., and Ferragina, C., 2007. "Intercalation compounds of  $\gamma$ -zirconium and  $\gamma$ -titanium phosphates 1,10-phenantroline copper complex materials." *Themochimica acta*, vol. 453, pp. 105-112.
- [7] La-Ginestra, A., Patrono, P., Beradelli, M. L., Golli, P., Ferragina, C., and Whittaker, D., 2000. *J. Mol. Cat.*, pp. 52187-52192.
- [8] Thakar, R. and Chudasama, U., 2009. "Synthesis, characterization and proton transport of crystalline zirconium titanium phosphates." *J. of Sci. and Ind. Res.*, vol. 68, pp. 312-318.
- [9] Alberti, G., Cherubini, F., and Palombari, R., 1996. "Preparation, proton transport and use in gas sensors of thin film zirconium phosphate with  $\gamma$ -layered structure." *Sensors and Actuators*, vol. 2, pp. 179-183.
- [10] Khan, A. A., Paquiza, L., and Khan, A., 2010. "An advanced nano-composite cation-exchanger polypyrrole zirconium phosphate as a Th(IV) selective potentiometric sensor." *J. of Mater. Sci.*, vol. 45, pp. 3610-3625.
- [11] Sun, L., Boo, W., Sun, D., Clearfield, A., and Sue, H. J., 2007. "Preparation of exfoliated epoxy/ $\alpha$ -zirconium phosphate containing high aspect ratio nanoplatelets." *Chem. Mater.*, pp. 1749-1754.
- [12] Feng, Y., He, W., Zhang, X., Jia, X., and Zhao, H., 2007. "The preparation of nanoparticle zirconium phosphate." *Mater Letters*, vol. 61, pp. 3258-3261.
- [13] Oyama, S. T. and Williams, S. M. S., 2011. "Inorganic polymeric and composite membranes." *Elsevier*, vol. 14,
- [14] Lin, Y. S. and Burggraaf, A. J., 1991. "Preparation and characterization of high temperature thermally stable alumina composite membrane." *J. Am. Ceramic Soc.*, vol. 140, pp. 361-364.
- [15] Lin, Y. S., de Vries, K. J., Brinkman, H. W., and Burggraaf, A. J., 1992. "Oxygen semipermeable solid oxide membrane composites prepared by electrochemical vapour deposition." *J. Membrane Science*, vol. 66, pp. 211-226.
- [16] Wang, H. B. and Lin, Y. S., 2012. "Effects of water vapour on gas permeation and separation properties of MFI zeolite membranes at high temperatures." *AIChEJ*, vol. 58, p. 15316.
- [17] Zhang, S. S., Xu, K., and Jow, T. R., 2005. "An inorganic composite membrane as the separator of Li-ion batteries." *J. of Power Sources*, vol. 140, pp. 361-364.
- [18] Shakshooki, S. K., El-Azzabi, O. H., Turki, F. M., El-Akari, F. A., Abodlal, R. J., and El-Tarhuni, S. R., 2012. "FT-IR and thermal behavior of  $\theta$ -type zirconium- and hafnium phosphates and the pellicular membranes." *Egypt J. of Anal. Chem.*, vol. 21, pp. 45-56.
- [19] Shakshooki, S. K., El-Azzabi, O. H., and Suliman, Y. A., 2013. "FT-IR spectra and thermal behavior of  $\alpha$ -vanadyl phosphate hemihydrate and its intercalated Mn<sup>2+</sup>, Ni<sup>2+</sup> and Zn<sup>2+</sup> metal ions." *The Libyan J. of Sci.*, vol. 17, pp. 23-31.
- [20] Ferragina, C. and Cafarelli, P., 1998. "53,  $\gamma$ -zirconium,  $\gamma$ -titanium phosphates platinum intercalate compound." *J of Thermal Anal*, vol. 53, pp. 189-206.
- [21] Yang, R., Qin, J., Li, M., Yanhong Liu, Y., and Fei Li, F., 2011. "Redox hydrothermal synthesis of cerium phosphate microspheres with different architectures." *Cryst., Eng. Comm.*, vol. 13,
- [22] Salvado, M. A., Pertierra, P., Tropajo, C., and Garcia, G. R., 2007. "Crystal structure of cerium (iv) bis (hydrogen phosphate derivative)." *J. Am. Chem. Soc.*, vol. 129, p. 10970.
- [23] Alberti, G. and Costantino, U., 1974. "Recent Progress in the Field of Synthetic Inorganic Exchanger Having a Layered and Fibrous Structure." *J. Chromatogr*, vol. 102, p. 5.
- [24] Parangi, T., Wani, P., and Chudasama, U., 2012. "Synthesis, Characterization and Application of Cerium Phosphate." *Desalination and Water Treatment*, vol. 38, p. 126.
- [25] Romano, R. and Alves, O. S., 2005. "Fibrous Cerium(IV) Phosphate Host of Weak and Strong Lewis Bases." *Inclus. Phenom. and Macrocyclic*, vol. 51, p. 211.
- [26] Casciola, M., Costantino, U., and Damico, S., 1988. "Conductivity of Cerium(IV) Phosphate in Hydrogen Form." *Solid State Ionics*, vol. 28, p. 617.
- [27] Varsheny, K. G., Tayal, N., Gupta, P., Agrawal, A., and Drabik, M., 2004. "Synthesis, Ion-Exchange and Physical Studies on Polystyrene Cerium(IV) Phosphate Hybrid Fibrous Ion Exchanger." *Ind. J. of Chem.*, vol. 43, p. 2586.
- [28] Metwally, S. S., El-Gammal, B., Ali, H. F., and Abo-EL-Enein, S. A., 2011. "Removal and separation of some radionuclides by poly-acrylamide based ce(IV) phosphate." *Separation Sci. and Tech*, vol. 46, p. 11.
- [29] Alberti, G., Casciola, M., Captani, D., Donnadio, A., Narducci, R., and Pica, M., 2007. "Novel Nafion-Zirconium phosphate composite membranes with enhanced stability of proton conductivity." *Electrochimica Acta*, vol. 52, p. 8125.
- [30] Yang, H. L., Lin, J. C. T., and Huang, C., 2009. "Application of nanosilver surface modification to RO membrane and spacer for mitigating biofouling in seawater desalination." *Water Research*, vol. 43, pp. 3777-3786.
- [31] Nagarale, R. K., Shin, W., and Singh, P. K., 2010. "Progress in Ionic Organic-Inorganic Composite Membranes for Fuel Cell Application." *Polym. Chem.*, vol. 1, p. 388.
- [32] Shakshooki, S. K., Elejmi, A. A., Khalfulla, A. M., and Elfituri, S. S., 2010. *Int. Conf. on Mater. Imperative*, vol. 11, pp. 49-70.

- [33] Bao, C., Gua, Y., Song, L., Lu, H., Yuan, B., and Hu, Y., 2011. "Facile synthesis of poly (vinyl alcohol)/ $\alpha$ -titanium phosphate nanocomposite with markedly enhanced properties." *Ind. Eng. Chem. Res.*, vol. 50, p. 11109.
- [34] Zhao, Y. H., Qian, Y. L., Zhu, B. K., and Xu, Y. Y., 2008. "Modification of porous poly(vinylidene fluoride) membrane using amphiphilic polymers with different structures in phase inversion process." *J. Membr. Sci.*, vol. 310, p. 567.
- [35] Beier, S. P., Enevoldsen, A. D., Kontogeorgis, G. M., Hansen, E. B., and Jonsson, G., 2007. "Adsorption of amylase enzyme on ultrafiltration membranes." *Langmuir*, vol. 23, p. 9341.
- [36] Hancock, L. F., Fagan, S. M., and Ziolo, M. S., 2000. "Hydrophilic semipermeable membranes fabricated with poly (ethylene oxide)-polysulfone block copolymer." *Biomaterials*, vol. 21, p. 725.
- [37] Li, Q., Mahendra, S., Lyon, D. Y., Brunet, L., Liga, M. V., Li, D., and Alvarez, P. J. J., 2008. "Antimicrobial nanomaterials for water disinfection and microbial control: potential applications and implications." *Water Res.*, vol. 42, p. 4591.
- [38] Vivien, W. W. B., Kenneth M. Y. Leung, J. W. Qiu, Michael H. W. Lam, , 2011. "Acute toxicities of five commonly used antifouling booster biocides to selected subtropical and cosmopolitan marine species." *Mar. Pollut. Bull.*, vol. 62, p. 1147.
- [39] Tenover, F. C., 2006. "Mechanisms of antimicrobial resistance in bacteria." *Am. J. Med.*, vol. 119, p. 3.
- [40] Kim, Y. H., Lee, D. K., Cha, H. G., Kim, C. W., and Kang, Y. S., 2007. "Synthesis and characterization of antibacterial Ag-SiO<sub>2</sub> nanocomposite." *J. Phys. Chem.*, vol. 111, p. 3629.
- [41] Chou, W. L., Yu, D. G., and Yang, M. C., 2005. "The preparation and characterization of silver loading cellulose acetate hollow fiber membrane for water treatment." *Polym. Adv. Technol.*, vol. 16, p. 600.
- [42] Deng, Y. Q., Dang, G. D., Zhou, H. W., Rao, X. H., and Chen, C. H., 2008. "Preparation and characterization of polyimide membranes containing Ag nanoparticles in pores distributing on one side." *Mater. Lett.*, vol. 62, p. 1143.
- [43] Damm, C., Munsted, H., and Rosch, H. A., 2007. "Long-term antimicrobial polyamide 6/silver nanocomposites." *J. Mater. Sci.*, vol. 42, p. 6067.
- [44] Basri, H., Ismail, A. F., Aziz, M., Nagai, K., Matsuura, T., Abdullah, M. S., and Ng, B. C., 2010. "Silver filled polyethersulfone membranes for antibacterial applications — effect of PVP and TAP addition on silver dispersion." *Desalination*, vol. 261, p. 264.
- [45] Basri, H., Ismail, A. F., and Aziz, M., 2011. "Polyethersulfone (PES)-silver composite UF membrane: effect of silver loading and PVP molecular weight on membrane morphology and antibacterial activity." *Desalination*, vol. 273, p. 72.
- [46] Duan, Y. Y., Jia, J., Wang, S. H., Yan, W., Jin, L., and Wang, Z. Y., 2007. "Preparation of antimicrobial poly ( $\epsilon$ - caprolactone) electrospun nanofibers containing silver-loaded zirconium phosphate nanoparticles." *J. Appl. Polym. Sci.*, vol. 106, p. 1208.
- [47] Choi, O., Deng, K. K., Kim, N. J., Ross, J. R. L., Surampalli, R. Y., and Hu, Z., 2008. "The inhibitory effects of silver nanoparticles, silver ions, and silver chloride colloids on microbial growth." *Water Research*, vol. 42, pp. 3066-3074.
- [48] Morones, J. R., Elechiguerra, J. L., Camacho, A., Holt, K., Kouri, J. B., Ramírez, J. T., and Yacaman, M. J., 2005. "The bactericidal effect of silver nanoparticles." *Nanotechnology*, vol. 16, pp. 2346-2353.
- [49] Hwang, E. T., Lee, J. H., Chae, Y. J., Kim, Y. S., Kim, B. C., Sang, B. I., and Gu, M. B., 2008. "Analysis of the toxic mode of action of silver nanoparticles using stress-specific bioluminescent bacteria." *Small*, vol. 4, pp. 746-750.
- [50] Siddhartha, S., Tanmay, B., Arnab, R., Gajendra, S., Ramachandrarao, P., and Debabrata, D., 2007. "Characterization of enhanced antibacterial effects of novel silver nanoparticles." *Nanotechnology*, vol. 18, p. 225103.
- [51] Jung, W. K., Koo, H. C., Kim, K. W., Shin, S., Kim, S. H., and Park, Y. H., 2008. "Antibacterial activity and mechanism of action of the silver ion in Staphylococcus aureus and Escherichia coli." *Appl Environ Microbiol.*, vol. 74, pp. 2171-2178.
- [52] Lok, C. N., Ho, C. M., Chen, R., He, Q. Y., Yu, W. Y., Sun, H., Tam, P. K., Chiu, J. F., and Che, C. M., 2006. "Proteomic analysis of the mode of antibacterial action of silver nanoparticles." *J Proteome Res.*, vol. 5, pp. 916-924.
- [53] Domènech, B., Muñoz, M., Muraviev, D. N., and J., M., 2013. "Polymer-Silver Nanocomposites as Antibacterial materials , Microbial pathogens and strategies for combating them: science, technology and education (A. Méndez-Vilas, Ed.)." *FORMATEX*,
- [54] Fang, M., Chen, J. H., Xu, X. L., Yang, P. H., and Hildebr, H. F., 2006. "Antibacterial activities of inorganic agents on six bacteria associated with oral infections by two susceptibility tests." *Int. J. Antimicrob. Agents*, vol. 27, pp. 513–517.